

Supporting Information

The theoretical comparison of different content of the third component in ternary organic solar cells

Ying Sun ^a, Li-Li Wang ^a, Jin-Hong Han ^a, Hai-Ping Zhou ^a, , Qing-Qing Pan ^{a,*}, Zhi-Wen Zhao ^{b,*}, Xing-Man

Liu ^c, Zhong-Min Su ^{a,d,*}

^aSchool of Chemistry and Environmental Engineering, Changchun University of Science and Technology, Jilin Provincial Science and Technology Innovation Center of Optical Materials and Chemistry, Jilin Provincial International Joint Research Center of Photo-functional Materials and Chemistry, Changchun, 130022, China

^bSchool of Materials Science and Engineering, Changchun University of Science and Technology, Changchun, 130022, China

^cSchool of Chemistry and Chemical Engineering, Ningxia University, Yinchuan 750021, China

^dState Key Laboratory of Supramolecular Structure and Materials, Institute of Theoretical Chemistry, College of Chemistry, Jilin University, Changchun 130021, China

Correspondence should be addressed to Q. Pan (panqq349@nenu.edu.cn) or Z. Zhao (zhaozw@hbuas.edu.cn) or Z. Su (zmsu@nenu.edu.cn)

Number of pages: 16

Number of Figs: 8

Number of tables: 3

Content

Simple introduction of General Amber Force Field and Marcus rate expression.

(Page S4)

Calculate interfragment charge transfer in electron excitation via interFragment Charge Transfer (IFCT).

(Page S5)

Fig. S1. Initial structure of **B1, Y7, BO-4Cl** molecule after optimization.

(Page S6)

Fig. S2. Process of MD simulations in **B1/Y7/BO-4Cl** blends and potential energy curve of the system at equilibrium in MD simulation. (The top group represents **B1:Y7 (10wt%):BO-4Cl** and the bottom group represents **B1:Y7 (50wt%):BO-4Cl**.)

(Page S6)

Fig. S3. The last step of NPT active layer snapshots and potential energy diagrams in **B1:Y7 (10wt%):BO-4Cl** and **B1:Y7 (10wt%):BO-4Cl**.

(Page S7)

Fig. S4. Proportion of different stacking patterns and stacking orientation for four group of binary complexes. ((a) is **B1:BO-4Cl-10wt%**, (b) is **B1:BO-4Cl-50wt%**, (c) is **B1:Y7-10wt%**, (d) is **B1:BO-4Cl-50wt%**.)

(Page S7)

Fig. S5. Probabilities of three stacking patterns at the D/A interface of the four groups of complexes.

(Page S8)

Fig. S6. CDD plots of the excited states S_1 , S_2 , S_3 of the four groups of binary complexes and the corresponding FE or CT or LE states.

(Page S8)

Fig. S7. Distributions of FE (FE_D and FE_A) and CT (FE/CT) states for the first twenty excited states of all binary complexes. ((a) for **B1:Y7 (10wt%):BO-4Cl** and (b) **B1:Y7 (50wt%):BO-4Cl**.)

(Page S8)

Fig. S8. (a) The ESP values of the donor and acceptor. (b) The ESP values of the vertical coordinate is the fragment of molecules, where the marked functional groups are the skeleton of donor, central core and IC of acceptors, respectively.

(Page S9)

Table S1. Relevant parameters of marcus theory.

(Page S9)

Table S2. Properties of binary complex with hot exciton mechanism.

(Page S10)

Table S3. Properties of binary complex with IEF mechanism.

(Page S12)

Reference

(Page S15)

General Amber Force Field : The general Amber force field (GAFF) uses 33 basic atom types and 22 special atom types covering almost all chemical spaces consisting of H, C, N, O, S, P, F, Cl, Br, and I.¹ Based on more than thousands of optimizations and single-point calculations by researchers, it has been verified as a complete force field, available for all parameters of the basic atom types.^{1,2} At present, it is widely used in the theoretical study of OSCs using GAFF for MD of the donor and acceptor, and the obtained data are consistent with the quantum calculations, which verifies the reliability of GAFF.³⁻⁷

Marcus rate expression: The charge transfer rate can be calculated by the semiempirical Marcus formula, Although we will follow convention in calling it Marcus theory⁸, the standard expression for non-adiabatic charge transfer between one donor D Although we will follow convention in calling it Marcus theory, the standard expression for non-adiabatic charge transfer between one donor D and one acceptor A was derived by Levich and Dogonadze:^{9,10}

$$k = \left(\frac{4\pi^2}{h}\right) V_{DA}^2 \left(\frac{1}{\sqrt{4\pi T \lambda K_B}}\right) \exp\left[-\frac{-(\Delta G + \lambda)^2}{4\lambda T K_B}\right]$$

Here, where h is Planck's constant, K_B is the Boltzmann constant, T with the temperature set to 298 K. V_{DA} , is D-A molecules interface electronic coupling, λ is recombination energy, including internal recombination (λ_{int}) and external recombination energy (λ_{ext}), ΔG is Gibbs free energy difference during the charge separation and charge recombination process. Where λ is the reorganization energy, V_{DA} represents electronic coupling, ΔG denotes the Gibbs free energy difference, h and k_B represent Planck and Boltzmann constants, respectively, and T is temperature. λ can be divided into internal recombination energy (λ_{int}) and external recombination energy (λ_{ext}), λ_{int} related to geometric changes to the donor and acceptor, λ_{ext} is influenced by the surrounding medium.^{10,11} We used the adiabatic potential surfaces proposed by Sun to calculate λ_{int} :¹²

$$\lambda_{int} = \lambda_1(A) + \lambda_2(D) = [E(A^-) - E(A)] + [E(D) - E(D^+)]$$

Where $E(A^-)$ and $E(A)$ are the energies of the neutral acceptor at the anionic geometry and optimal ground-

state geometry, and $E(D)$ and $E(D^+)$ are the energies of the radical cation at the neutral geometry and optimal cation geometry.

The λ_{ext} can be defined by:¹³

$$\lambda_{ext} = \left(\frac{1}{4\pi\epsilon_0} \right) \Delta e^2 \left(\frac{1}{2a_1} + \frac{1}{2a_2} - \frac{1}{R} \right) \left(\frac{1}{\epsilon_{OP}} - \frac{1}{\epsilon_0} \right)$$

Where ϵ_{op} and ϵ_0 are the optical dielectric and static dielectric constants, respectively, a_1 and a_2 are the effective radius of the donor and acceptor, R is the center distance between donor and acceptor.

V_{DA} can be estimated by the generalized Mulliken-Hush (GMH) formalism as follows, which involves a vertical transition from the initial to the final state.^{14,15}

$$V_{DA} = \frac{\Delta E \mu_{tr}}{\sqrt{(\Delta\mu)^2 + 4(\mu_{tr})^2}}$$

Where μ_{tr} is the transition dipole moment between the ground state and the excited state, $\Delta\mu$ is the difference of the dipole moment between two states, and ΔE is the energy difference.

The Gibbs free energy difference in the processes of charge transfer and recombination can be approximate estimated by Rehm–Weller formula.^{16,17}

$$\Delta G_{CS} = E_{EA}(A) - E_{IP}(D) - \Delta E_{S1} - \Delta E_b$$

$$\Delta G_{CR} = E_{IP}(D) - E_{EA}(A)$$

Where $E_{EP}(A)$ and $E_{IP}(D)$ correspond to the electron affinity of acceptor and ionization potential of donor, respectively, which can be calculated approximately by the HOMO energy level of donor and LUMO of acceptor,¹⁸ ΔE_{S1} is the energy of lowest excited state for the donor, and E_b is exciton binding energy. It's worth noting that the estimation of Gibbs free energy is related to the LUMO energy levels of individual donor and acceptor, which are still hard to get a precise value both in experimental and theoretical aspects.

Calculate interfragment charge transfer in electron excitation via interFragment Charge Transfer (IFCT):

The IFCT method contains three steps: (i) Calculating atomic contribution to hole and electron. (ii) Calculating

fragment contributions to hole and electron by summing up atomic contributions. (iii) Constructing interfragment charge transfer matrix \mathbf{Q} . Its (R,S) element corresponds to the electron transfer from fragment R to fragment S during the excitation:

$$Q_{R,S} = \Theta_{R,\text{hole}} \Theta_{S,\text{ele}}$$

where $\Theta_{R,\text{hole}}$ and $\Theta_{S,\text{ele}}$ denote contribution of fragment R to hole and contribution of fragment S to electron, respectively. Above formula is very easy to comprehend, it essentially assumes that electron transfer from R to S is proportional to both composition of R in hole (where electron leaves) and composition of S in electron (where electron goes).

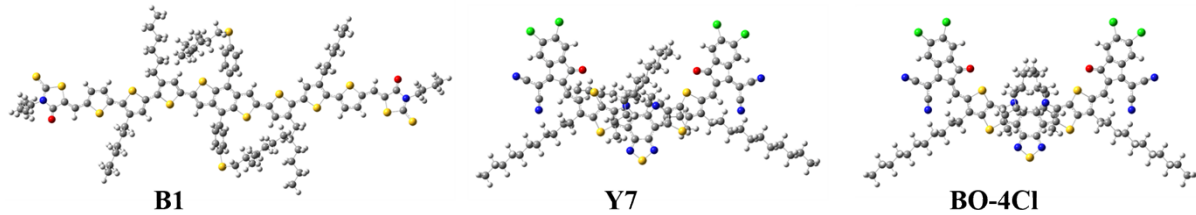


Fig. S1. Initial structure of **B1**, **Y7**, **BO-4Cl** molecule after optimization.

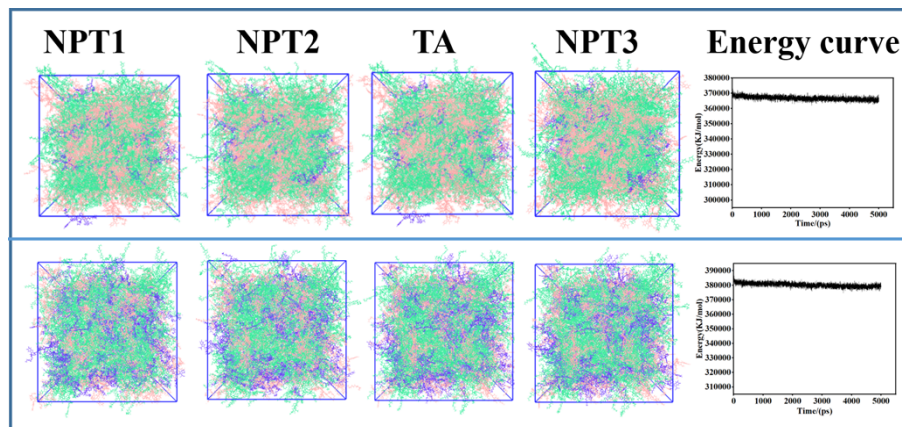


Fig. S2. Process of MD simulations in **B1/Y7/BO-4Cl** blends and potential energy curve of the system at equilibrium in MD simulation. (The top group represents **B1:Y7 (10wt%):BO-4Cl** and the bottom group represents **B1:Y7 (50wt%):BO-4Cl**.)

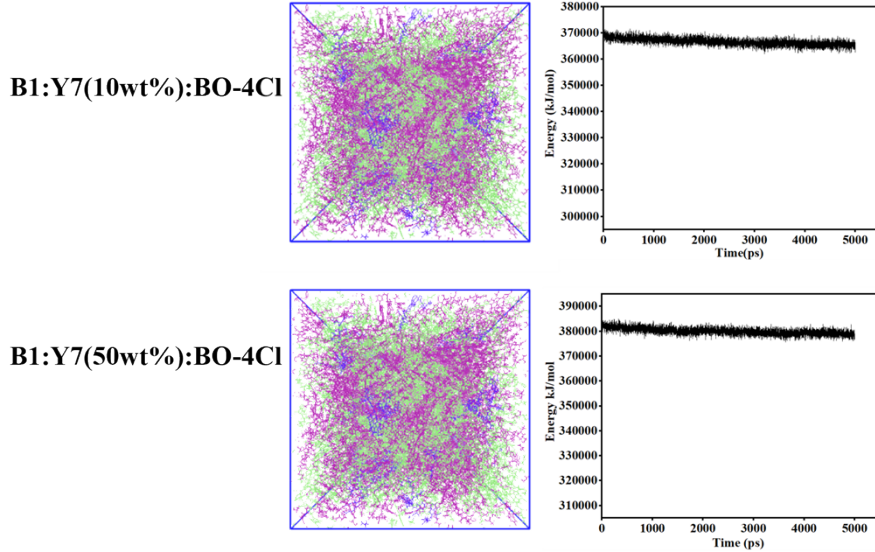


Fig. S3. The last step of NPT active layer snapshots and potential energy diagrams in **B1:Y7 (10wt%):BO-4Cl** and **B1:Y7 (10wt%):BO-4Cl**.

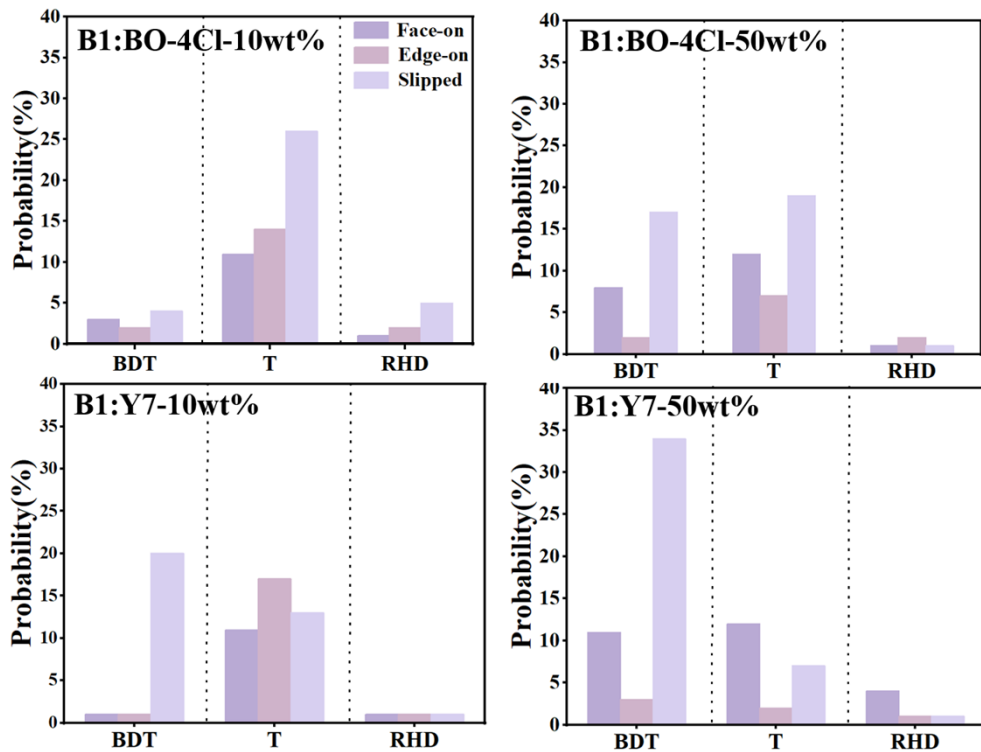


Fig. S4. Proportion of different stacking patterns and stacking orientation for four group of binary complexes. ((a) is **B1:BO-4Cl-10wt%**, (b) is **B1:BO-4Cl-50wt%**, (c) is **B1:Y7-10wt%**, (d) is **B1:BO-4Cl-50wt%**.)

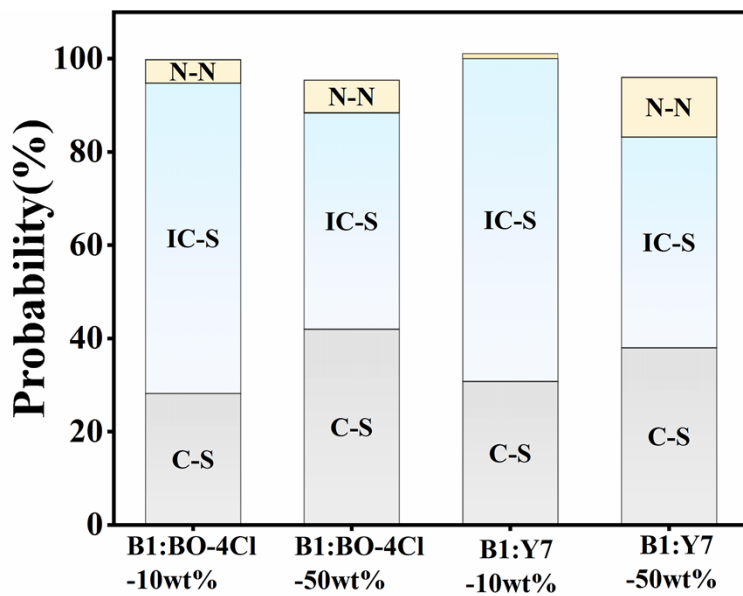


Fig. S5. Probabilities of three stacking patterns at the D/A interface of the four groups of complexes.

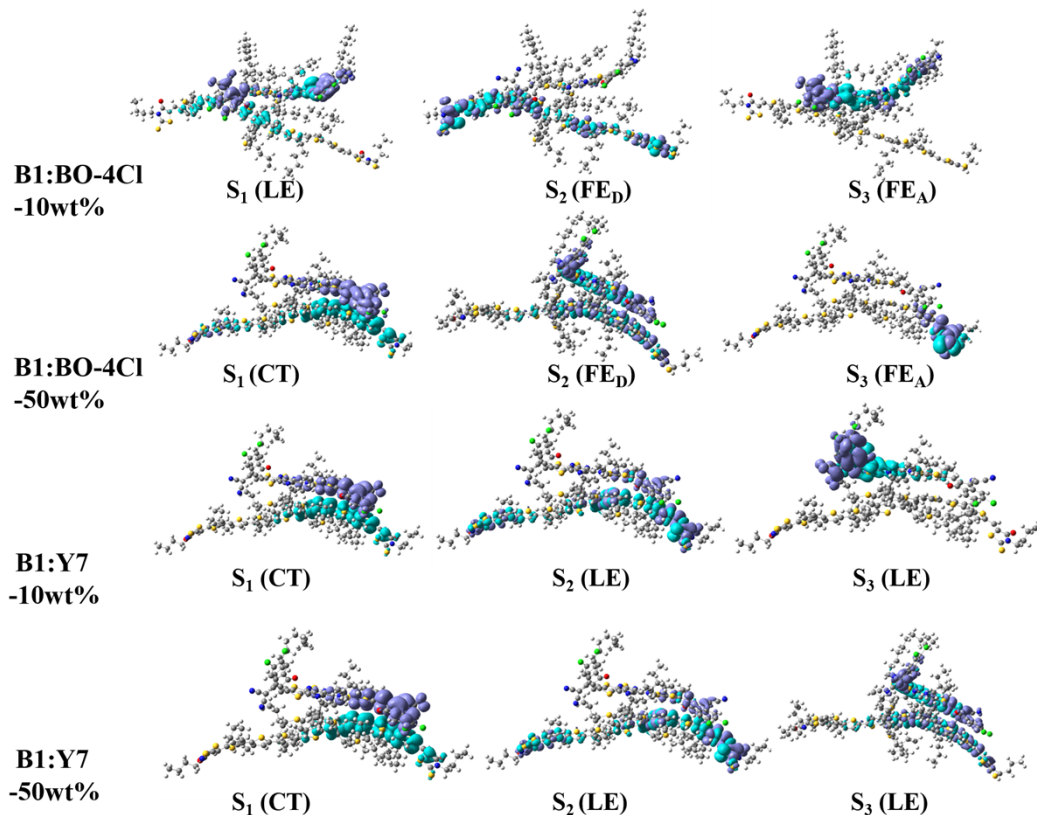


Fig. S6. CDD plots of the excited states S₁, S₂, S₃ of the four groups of binary complexes and the corresponding FE or CT or LE states.

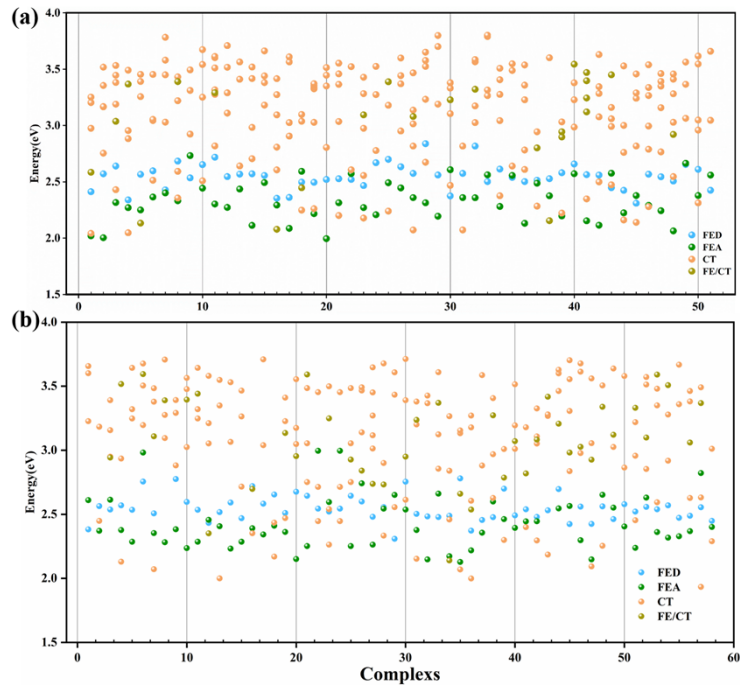


Fig. S7. Distributions of FE (FE_D and FE_A) and CT (FE/CT) states for the first twenty excited states of all binary complexes. ((a) for B1:Y7 (10wt%):BO-4Cl and (b) B1:Y7 (50wt%):BO-4Cl.)

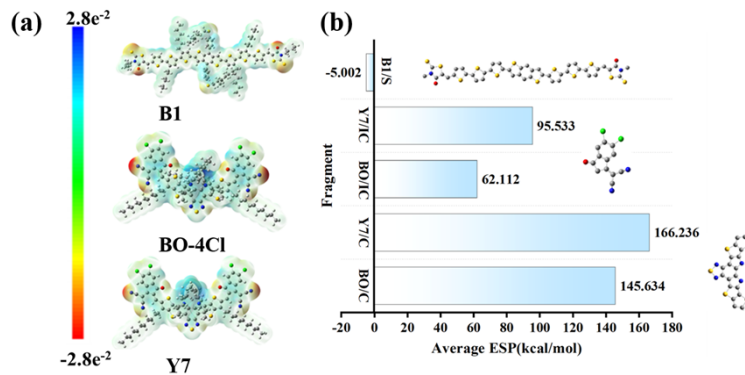


Fig. S8. (a) The ESP values of the donor and acceptor. (b) The ESP values of the vertical coordinate is the fragment of molecules, where the marked functional groups are the skeleton of donor, central core and IC of acceptors, respectively.

Table S1. Relevant parameters of marcus theory.

System	λ_{int}	λ_{ext}	ΔG_{CS}
--------	------------------------	------------------------	------------------------

B1:BO-4Cl_10wt%	0.2936	0.2983	-0.7998
B1:BO-4Cl_50wt%			
B1:Y7_10wt%	0.2934	0.3014	-0.7867
B1:Y7_50wt%			

Table S2. Properties of binary complex with hot exciton mechanism.

In **B1:BO-4Cl-10wt%**

Complex	E_{CT} (eV)	f	E_{FED}	f	E_{FED-CT} (eV)
1	2.2839	0.0001	2.5138	3.0212	0.2299
2	2.1545	0.0067	2.6753	0.8697	0.5208
3	2.2483	0.1957	2.4971	2.8067	0.2488
4	2.5133	0.0002	2.5970	3.5948	0.0837
5	2.0417	0.0062	2.4123	3.0578	0.3706
6	2.3563	0.1877	2.6835	2.6163	0.3272
7	2.0473	0.0154	2.3391	3.4006	0.2918
8	2.1327	0.0001	2.5658	3.3676	0.4331
9	2.2340	0.0104	2.6730	3.022	0.4390
10	2.2395	0.0300	2.6994	3.5526	0.4599
11	2.6736	0.0009	2.8382	1.5224	0.1646
12	2.3084	0.0002	2.7527	2.9892	0.4443
13	2.0724	0.0142	2.5743	3.8286	0.5019
14	2.3759	0.0269	2.6131	3.2253	0.2372
15	2.2608	0.0002	2.4948	3.2470	0.2340

16	2.2007	0.0704	2.5269	1.8833	0.3262
17	2.1780	0.1002	2.4664	3.3329	0.2884
18	2.5564	0.0000	3.1811	3.7566	0.6247
19	2.5020	0.0001	3.2649	0.4954	0.7629
20	2.0212	0.0003	2.9082	3.2102	0.887

In **B1:BO-4Cl-50wt%**.

Complex	E_{CT} (eV)	f	E_{FED}	f	E_{FED-CT} (eV)
1	2.1293	0.1266	2.5697	2.6851	0.4404
2	2.0708	0.0677	2.5071	4.1227	0.4363
3	2.1697	0.0205	2.6541	3.0929	0.4844
4	2.1521	0.0003	2.5033	3.3038	0.3512
5	1.9994	0.1297	2.4173	2.5424	0.4179
6	2.4484	0.0442	2.5635	4.8593	0.1151
7	2.3521	0.0516	2.7199	2.924	0.3678
8	2.2629	0.0007	2.5438	3.1278	0.2809
9	2.4699	0.0316	2.811	0.7163	0.3411
10	2.3333	0.1344	2.5746	2.6688	0.2413
11	2.5556	0.1674	2.5776	2.5431	0.022

In **B1:Y7-10wt%**.

Complex	E_{CT} (eV)	f	E_{FED}	f	E_{FED-CT} (eV)
1	2.3218	0.1962	2.5805	3.4179	0.2587
2	2.9662	0.0008	3.0460	2.9233	0.0798

3	2.1613	0.1061	2.4244	2.8169	0.2631
4	2.4991	1.016	2.5599	2.3959	0.0608
5	2.3486	0.0286	2.5628	2.7652	0.2142
6	2.3126	0.0619	2.6106	3.9108	0.2980
7	2.2796	0.0009	2.5677	3.7010	0.2881
8	2.1400	0.0006	2.3097	0.8953	0.1697

In **B1:Y7-50wt%**.

Complex	E_{CT} (eV)	f	E_{FED}	f	E_{FED-CT} (eV)
1	2.2538	0.0009	2.5618	2.8845	0.308
2	2.0926	0.0063	2.425	2.2810	0.3324
3	2.4595	0.7618	2.4885	3.0893	0.029
4	2.0696	0.0025	2.5802	0.7122	0.5106
5	1.9991	0.0185	2.3717	3.2079	0.3726
6	2.2999	0.0105	2.5998	3.1137	0.2999
7	2.2952	0.0301	2.4788	1.8589	0.1836
8	2.4535	0.1411	2.5205	3.3616	0.067
9	2.3349	0.1822	2.5801	2.4750	0.2452
10	2.2894	0.0000	2.4484	3.0038	0.159
11	2.3993	0.0000	2.5383	3.0682	0.139
12	2.3331	0.0614	2.4544	2.9269	0.1213

Table S3. Properties of binary complex with IEF mechanism.

In **B1:BO-4Cl-10wt%**.

Complex	E_{CT} (eV)	f	E_{FED}	f	E_{FED-CT} (eV)
1	2.3563	0.1877	2.3314	0.5088	-0.0249
2	2.5084	0.0022	2.4432	0.9673	-0.0652
3	2.6407	0.0477	2.5683	2.8024	-0.0724
4	2.2608	0.0372	2.2168	1.6384	-0.0440
5	3.1896	0.0000	3.1181	3.4150	-0.0715
6	2.4680	0.0238	2.3744	2.4579	-0.0936
7	3.0258	0.0004	2.9665	3.3238	-0.0593

In **B1:BO-4Cl-50wt%**.

Complex	E_{CT} (eV)	f	E_{FED}	f	E_{FED-CT} (eV)
1	2.4484	0.0442	2.3705	2.8845	-0.0079
2	3.0247	0.0103	2.9921	0.7263	-0.0326
3	2.6130	2.7378	2.5371	3.1137	-0.0759

In **B1:Y7-10wt%**.

Complex	E_{CT} (eV)	f	E_{FED}	f	E_{FED-CT} (eV)
1	2.5635	0.0442	2.4484	2.8593	-0.0779
2	2.5556	0.0077	2.5073	1.5031	-0.0483

In **B1:Y7-50wt%**.

Complex	E_{CT} (eV)	f	E_{FED}	f	E_{FED-CT} (eV)
1	2.5599	1.0160	2.4991	2.3959	-0.0608

2	2.2241	0.1061	2.1613	2.8169	-0.0628
3	2.2097	0.0026	2.1400	0.8953	-0.0697
4	2.2917	0.0229	2.2796	0.7918	-0.0121
5	2.3778	0.0619	2.3126	0.9177	-0.0652

References

1. J. Wang, R. M. Wolf, J. W. Caldwell, P. A. Kollman, D. A. Case, *J. Comput. Chem.*, 2004, 25, 1157-1174
2. G. C. Han, Y. Guo, X. Y. Ma, Y. P. Yi, *Sol. RRL.*, 2018, 2, 1800190
3. M. Y. Li, Y. Ren, J. C. Huang, M. Y. Sui, G. Y. Sun, Z. M. Su, *J. Mater. Chem. A.*, 2022, 10, 22477-22487
4. J. Yang, W. L. Ding, Q. S. Li, Z. S. Li, *J. Phys. Chem. Lett.*, 2022, 13, 916-922
5. Q. Q. Pan, S. B. Li, Y. C. Duan, Y. Wu, J. Zhang, Y. Geng, L. Zhao, Z. M. Su, *Phys. Chem. Chem. Phys.*, 2017, 19, 31227-31235
6. Z. Wang, G. C. Han, L. Y. Zhu, Y. Guo, Y. P. Yi, Z. G. Shuai, Z. X. Wei, *Phys. Chem. Chem. Phys.*, 2018, 20, 24570-24576
7. J. Yang, Q. S. Li, Z. S. Li, *Colloids Surf. A.*, 2023, 659, 130818
8. R. A. Marcus, *J. Chem. Phys.*, 1956, 24, 966
9. V. Levich and R. Dogonadze, *Dokl. Akad. Nauk. SSSR*, 1959, 124, 123-126
10. N.B. Taylor, I. Kassal, *Chemical Science*, 2018, 9 (11), 2942-2951
11. A. Burquel, V. Lemaur, D. Beljonne, R. Lazzaroni, J. Cornil, *J. Phys. Chem. A.*, 2006, 110, 3447-3453
12. V. Lemaur, M. Steel, D. Beljonne, J. L. Brédas, J. Cornil, *J. Am. Chem.*, 2005, 127, 6077-6086
13. Y. Z. Li, T. Pullerit, M.Y. Zhao, M.T. Sun, *J. Phys. Chem. C.*, 2011, 115, 21865-21873
14. Y. A. Duan, Y. Geng, H. B. Li, J. L. Jin, Y. Wu, Z. M. Su, *J. Comput. Chem.*, 2013, 34, 1611-1619
15. H. P. Hsu, *Acc. Chem. Res.*, 2009, 42, 509-518
16. A. A. Voityuk, *J. Chem. Phys.*, 2006, 124, 064505
17. V. M. Geskin, F. C. Grozema, L. D. A. Siebbeles, D. Beljonne, J. L. Brédas, J. Cornil, *J. Phys. Chem. B*, 2005, 109, 20237-20243
18. P. K. Das, A. J. Muller, G. W. Griffin, I. R. Gould, C. H. Tung, N. J. Turro, *Photochem. Photobiol.*, 1984, 39, 281-285

19. X. Zhang, L. Chi, S. M. Ji, Y. B. Wu, P. Song, K. L. Han, H. M. Guo, T. D. James, J. Z. Zhao, *J. Am. Chem. Soc.*, 2009, 131, 17452-17463